Sigma J Eng & Nat Sci 38 (3), 2020, 1099-1112

Sigma Journal of Engineering and Natural Sciences
Sigma Mühendislik ve Fen Bilimleri Dergisi

Research Article

STATISTICAL MODELLING OF THE ADSORPTIVE DEPHENOLATION OF PETROLEUM INDUSTRY WASTEWATER USING IONIC LIQUID TREATED CLAY

Matthew N. ABONYI[1], Chukwunonso O. ANIAGOR*[2], Matthew Chukwudi MENKITI[3]

[1]*Chemical Eng. Department, Nnamdi Azikiwe University, Awka, NIGERIA;* ORCID: 0000-0002-5876-4885
[2]*Chemical Eng. Department, Nnamdi Azikiwe University, Awka, NIGERIA;* ORCID: 0000-0001-6488-3998
[3]*Chemical Eng. Department, Nnamdi Azikiwe University, Awka, NIGERIA;* ORCID: 0000-0001-8552-3756

Received: 26.11.2019 Revised: 16.01.2020 Accepted: 16.01.2020

ABSTRACT

In this paper, response surface methodology (RSM) was employed in modelling and optimizing the adsorption characteristics of phenol unto ionic liquid-based hybrid clay (IL-C). The effect of adsorbent dosage, contact time, effluent temperature and effluent pH as independent variables were studied; while removal efficiency was considered as the response variable. Second-order polynomial regression model successfully elucidated the effect of the independent variables on the dephenolation process. A coefficient of determination (R^2) value of 0.98, model F-value of 83.52, P-value (< 0.0001) and low value of the coefficient of variation (0.81%) corroborates the suitability of second-order polynomial regression model. Furthermore, the optimization result showed that the optimum operating conditions for realizing the maximum removal efficiency (91.67 %) were; 25 min, 40 ^{0}C, pH 6.6 and 1.5g adsorbent mass.

Keywords: Adsorption, dephenolation, response surface methodology, ionic liquid, clay, statistical modelling.

1. INTRODUCTION

Phenols and its derivatives are useful raw materials in coal/petroleum refining, pharmaceuticals, pulp & paper, tannery and petrochemical industries [1]**.** Consequently, phenol laden effluents generated by these process industries, when released to the environment could pose a serious potential hazard for aquatic life and human health. Thus, the US environmental protection agency (USEPA) enlisted phenol as priority pollutant, with a permissible limit of 0.1 mg/l in wastewater [2]. Considering the hazards associated with phenol contamination of aquatic environments, there is the need for effective dephenolation of relevant industrial effluent before their discharge into the environment.

According to Ahmaruzzaman, [3], solvent extraction, biodegradation, distillation, and membrane separation are some of the commonly adopted approaches in dephenolation operation. However, these methods are not without some drawbacks, some of which are cost

* Corresponding Author: e-mail: aniagor@yahoo.com, tel: +234 -8061232153

incompatibility, high sludge production and poor removal efficiency [4]. Song, et al. [5] reported that adsorption technique is often preferred in effluent dephenolation due to its relative operational flexibility, the simplicity of its design and its cost-effectiveness. The use of commercial/low-cost activated carbon, lignite and acid/salt treated-clay as adsorbents has been reported [6].

Though some research works exist in the field of dephenolation using chemically modified clay as adsorbe nts [7 - 8], a detailed investigation and modelling of the dephenolation process using optimization tool are necessary. Such necessity forms the motivation and basis for this paper. Hence, the distinct objective of this work is to synthesize ionic liquid-based hybrid clay (IL-C) and to statistically model, as well as optimize the process variables to establish the optimum dephenolation conditions.

Notably, process variable optimization is paramount for effective design of an adsorption system. The conventional optimization technique for a multivariable system involving the one-factor at a time (O-F-A-T) approach may not be entirely tedious. However, the approach (O-F-A-T) is prone to non-reliability of obtained results, non-depiction of the interaction effects of the independent variables and time ineffectiveness due to the existence of multiple experimental runs [9]. These limitations can be eliminated by optimizing all the variables collectively via statistical experimental design afforded by response surface methodology (RSM). RSM, a collection of mathematical and statistical techniques is a useful tool for the modelling and analyses of problems relating a response of interest, as influenced by several independent variables [10]. To achieve efficient model prediction, prior knowledge of the process being investigated was necessary. Despite the prevalent use of RSM in optimizing chemical processes and to our best knowledge, no optimization study on dephenolation of wastewater from petroleum industry using IL-C has been reported; thus making this work imperative.

2. METHODS

2.1. Material collection and ionic liquid synthesis

The petroleum effluent sample used in the study was sourced from dehydrator point of an oil facility in Warri, Nigeria. The collected sample was preserved in a concentrated sulphuric acid medium to maintain its integrity. The adsorbent precursor (clay sample) was obtained from Nteje (Long. 6.55^{o}E, Lat. 6.16^{o}N), Anambra State, Nigeria.

The ionic liquid (1-ethyl-3-methylimidazolium bromide, EMIB) used for the hybrid treatment of the clay sample was synthesized via the procedure reported by Wilkes and Zaworotko, [11], with slight modifications as stated herein. 2-methylimidazole (8.91 g), acetonitrile (70 ml) and acetone (40 ml) were charged into a 250 ml flat-bottomed flask; with the mixture heated for 10 min at 60 ^{0}C. Afterwards, bromo-ethane (3 ml) was introduced into the flask followed by distillation of the entire mixture at 80^{0}C for 15 min. 1-ethyl-3-methylimidazolium bromide (EMIB), obtained as a bottom product from distillation was allowed to flow through silica gel to remove any unreacted salt and colour. Other useful chemicals for this study are all of the analytical grades, purchased from Onitsha chemical and reagent store.

2.2. Adsorbent synthesis

The collected clay sample was air-dried, mechanically ground to uniform particle size and afterwards, activated thermally at 200 ^{0}C for 2 h. The resultant heat treated clay (HTC) sample was then cooled and stored in airtight containers, ready for further chemical treatment. For the chemical treatment, suitable volume (based on the dry weight of HTC) of already synthesized ionic liquid (EMIB) was measured into 1000 ml beaker containing the HTC. The mixture was allowed to stand for 1 h with intermittent stirring to ensure the formation of homogenous slurry.

After 1 h, the slurry was air-dried and the resultant clay pellets (ionic liquid-based hybrid clay, IL-C) was mechanically crushed. Using pa rticle size distribution analyzer, various particle size ranges (150, 300 and 600 μm) were obtained and stored separately for use.

2.3. Preliminary batch adsorption experiment

In the preliminary batch adsorption experiment, a specified amount of IL-C of uniform particle size was added to 50 ml of petroleum effluent (of known concentration, pH and temperature) contained in 250 ml conical flask. Using temperature-controlled magnetic stirrer (at 50 rpm), the mixture was constantly agitated. Test samples were withdrawn from the set-up at varying time intervals until attainment of equilibrium. The drawn samples (at the respective time intervals) were collected in a separate sample bottle and allowed to cool. The absorbances of the supernatants were analyzed using UV-VIS spectrophotometer at 270 nm.

Above procedure was adopted for studying the effects of the various process variables on the dephenolation operation as stated herein. The effect of solution temperature was studied over a range of 25 – 60 ^{0}C, while the other process parameters were kept constant. For the effect of adsorbent dosage, 50 ml of the effluent (at a constant temperature, pH and particle size) was contacted with varying adsorbent masses (1.0, 1.5, 2.0 and 2.5 g). The effect of effluent dephenolation time was studied at 5 min intervals within the time range 5 to 35 min, with the rest variables kept constant. The pH effect was investigated over the range of pH 4.0 – pH 10.0. The effluent pH was adjusted using 0.1 N HCl and NaOH (as applicable). The amount of phenol adsorbed at equilibrium, q_e and at time t, q_t were calculated using Eqs. (1 – 2)**;**

$$q_e = \frac{(C_o - C_e)V}{W} \quad (1)$$

$$q_t = \frac{(C_o - C_t)V}{W} \quad (2)$$

Where q_e is the equilibrium adsorption capacity per gram of dry weight of the adsorbent, (mg/g); q_t is the adsorption capacity at the time, t (mg/g); C_o is the initial concentration of phenol in the solution (mg/l); C_e is the final or equilibrium concentration of phenol in the solution (mg/l); C_t is the amount of phenol adsorbed at time t (mg/l); V is the volume of the solution (L); W is the dry weight of adsorbent (g). The percentage dephenolation efficiency RE (%) was calculated using Eq. 3 [12]**;**

$$RE(\%) = \frac{C_o - C_e}{C_o} \times 100 \quad (3)$$

2.4. Experimental design

The central composite design (CCD) was used for the experimental design and to study the interaction effects of the dephenolation process variables. In using CCD, linear, quadratic, cubic and cross-product effects of the process variables on the dephenolation efficiency were investigated. Contact time (X_1), effluent temperature (X_2), adsorbent dosage (X_3) and effluent pH (X_4) were the identified set of independent process variables. Meanwhile, their influences on the output variable (% dephenolation efficiency) were investigated. Design Expert v.8.0 software was used for the design of the experiment. For a design of four independent variables (n = 4), each with two different levels, the total number of experiments (N) was worked out as; $N = (n^2 + 2n + n_c) = 16 + (2 \times 4) + 6 = 30$. This includes the standard 2n factorial points with their origin at the centre; '2n' axial points fixed at a distance 'α' from the centre to generate the quadratic terms, and 'n_c' replicate points at the centre. After defining the range of each of the process variables, they were coded to lie at ± 1 for the factorial points, '0' for the centre points, and ±α for the axial points. The numerical values of the variables were transformed into their respectively coded values as shown in Eq. 4:

$$X_i = \frac{2X-(X_{max}-X_{min})}{X_{max}-X_{min}} \quad (4)$$

Where X_i is the required coded value of a variable; X, X_{min} and X_{max} are the low and high values of X, respectively. The selected process variables with their limits, units and notations are given in Tables 1, while the experimental design matrix for the process is presented in Table 2. The output variable/response (Y) was used to develop an empirical model that depicts its (response, Y) with the selected independent variable using a second-order polynomial equation given by Eqn. 5 [13]**;**

$$Y = \beta_o + \sum_{i=1}^{n} \beta_i X_i + \sum_{i=1}^{n} \beta_{ii} X_i^2 + \sum_{i=1}^{n} \sum_{j=1}^{n-1} \beta_{ij} X_i X_j \quad (5)$$

Where *Y* is the predicted response, β_o is the constant coefficient, β_i is the linear coefficient, β_{ij} is the interaction coefficient, β_{ii} is the quadratic coefficient, and X_i, are the coded values for the factors.

Table 1. Experimental range and levels of the independent variables for phenol uptake

		Codes	Variable	Level		
Variables	Code	$-\alpha$	-1	0	+1	$+\alpha$
Time (min)	X_1	5	11.273	50	28.727	35
Temp (^{0}C)	X_1	25	32.381	75	52.681	60
Dosage (g)	X_3	0.5	0.918	1.5	2.082	2.5
pH	X_4	4	5.256	8.5	8.745	10

Table 2. Experimental design for dephenolation of petroleum effluent

STD	Process variables				Response variables	
	Time (X_1)	Temp.(X_2)	Dosage (X_3)	pH (X_4)	Observed	Predicted
1	15.00	30.00	1.00	5.00	89.90	89.90
2	25.00	30.00	1.00	5.00	88.79	90.36
3	15.00	50.00	1.00	5.00	93.74	93.22
4	25.00	50.00	1.00	5.00	91.87	91.88
5	15.00	35.00	2.00	5.00	81.20	83.67
6	25.00	30.00	2.00	5.00	89.87	87.82
7	15.00	50.00	2.00	5.00	91.46	90.02
8	25.00	50.00	2.00	5.00	90.71	91.83
9	15.00	30.00	1.00	8.00	97.35	96.70
10	25.00	30.00	1.00	8.00	94.56	93.31
11	15.00	50.00	1.00	8.00	98.54	96.92
12	25.00	50.00	1.00	8.00	95.39	94.72
13	15.00	30.00	2.00	8.00	88.41	87.09
14	25.00	35.00	2.00	8.00	87.07	88.09
15	15.00	50.00	2.00	8.00	93.26	93.51
16	25.00	50.00	2.00	8.00	92.87	92.11
17	12.93	40.00	1.50	6.50	95.44	95.11
18	27.02	40.00	1.50	6.50	93.66	94.38
19	20.00	35.86	1.50	6.50	89.20	88.79
20	20.00	54.14	1.50	6.50	93.12	93.92
21	20.00	40.00	0.79	6.50	98.50	98.50
22	20.00	35.00	2.21	6.50	91.76	92.17
23	20.00	35.00	1.50	4.38	95.81	95.94
24	20.00	30.00	1.50	6.25	97.34	98.41
25	20.00	40.00	1.50	6.50	98.76	98.41
26	20.00	40.00	1.50	6.50	98.75	98.41
27	20.00	40.00	1.50	6.50	98.75	98.41
28	20.00	40.00	1.50	6.50	98.77	98.41
29	20.00	40.00	1.50	6.50	98.76	98.41
30	20.00	40.00	1.50	6.50	98.76	98.41

3. RESULTS AND DISCUSSION

3.1. Instrumental Characterization of adsorbent

3.1.1. Surface morphology

The surface morphologies of the unloaded and phenol-loaded IL-C are shown in Figs.1(a-b). A coarse and loosely packed structure, with evidence for the existence of flake-like and irregular edges, characterized the unloaded IL-C (Fig 1a). Also, large and well-developed pore was observed in Fig 1(a). These observations could be a consequence of the physical process involved in the ionic liquid binding onto the thermally activated clay particles to produce the adsorbent (IL-C). In contrast, the interstitial pore spaces previously existent on the unloaded IL-C (Fig 1a) were remarkably absent in Fig 1(b). The probable presence of the adsorbed phenol molecules, which tends to occupy and fill-up these void spaces on the adsorbent, could be the obvious explanation

to aforestated observation. Therefore, it could be concluded that the structural defect entrenched on the thermally activated clay during chemical modification significantly enhanced IL-C pore development.

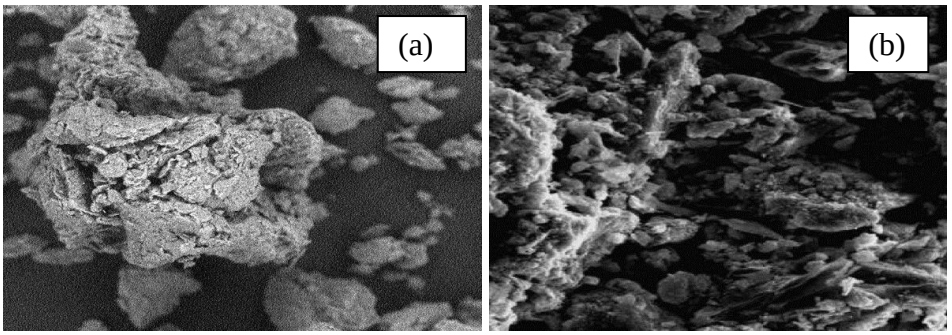

Figure 1. SEM of IL-C (a) before adsorption (b) after adsorption

3.1.2. Surface chemistry

In this study, the surface chemistry of unloaded and phenol-loaded IL-C was performed via FTIR analyses and presented in Figs. 2 (a-b). Functional groups were assigned to the various discernable wave-numbers/peaks on the FTIR spectra, with the due recourse of the standard signature in the FTIR library presented by Stuart, [14]. The prevalent peaks for unloaded IL-C (Fig 2a) were found at wave-numbers 2922.2, 2855.1, 1461.1, 1375.4 and 723.1 cm^{-1}. The peak at 2992.2 cm^{-1} is assigned to Si - O stretching, thus suggesting the kaolinite nature of the clay sample [15]. The peak at 2855.1 cm^{-1} is attributed to N-H stretching vibration of ammonium ion originating from the ionic liquid used for the chemical treatment of heat-treated clay (HTC) sample. The presence of trivalent (Al^{3+}, Fe^{3+}) or divalent (Mg^{2+}) ions substitution on the octahedral sheet of the HTC charge layers is highlighted by the peaks around 1500 – 1300 cm^{-1}. Furthermore, the peak at 723.1 cm^{-1} is assigned to halogen–carbon stretching (C-Br) group originating from the ionic liquid treatment of the HTC. Meanwhile, this incorporation of this halogen group to the existent HTC aliphatic bond strengthened it due to the high transmittance (90.27%) recorded at that wave-number.

A comparison of the FTIR spectra of the unloaded (Fig 2a) and phenol-loaded IL-C (Fig 2b) showed the appearance of few peaks and variation in the % transmittance of existent peaks, accompanied with an obvious shift in their respective wave numbers. The involvement of the affected functional groups in the adsorption process is the possible explanation to aforestated observations. For instance, the % transmittance of the peaks at 2922.2 and 2855.1 cm^{-1} changed from 50.164 and 62.691 %, respectively (before adsorption) to 80.477 % and 83.220 %, respectively (after phenol adsorption). This improvement in % transmittance implies a limited number of the available bond (due to their involvement in the adsorption process) for absorbing the coloured light transmitted through the sample. Similarly, the peaks at wave-numbers 1461.1 and 1375.4 cm^{-1} (for unloaded IL-C) shifted to 1457.4 and 1384.2 cm^{-1}, respectively after adsorption. The observed shift from a higher wave-number of 1461.1cm^{-1} to a lower wave-number of 1457.4cm^{-1} implies a reduction in the adsorbent mass due to the possible elimination of certain chemical bonds during adsorption [16]. Similarly, an increment in wave-number from 1375.4 cm^{-1} to 1384.2 cm^{-1} depicts the existence of a larger adsorbent mass after adsorption. This increase in mass could be due to the presence of adsorbed phenolic ions on the adsorbent [16]**.** Furthermore, the detection of new peaks at wave-numbers 991.5 and 3235.5 cm^{-1} attest to the formation of relevant post-adsorption bonds.

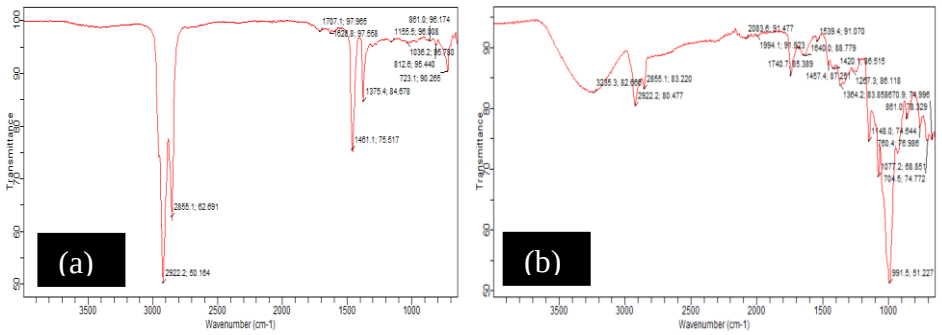

Figure 2. FT-IR spectra of IL-C (a) before adsorption (b) after adsorption

3.1.3. Identification of EMIB by GC-MS

The mass spectrum of the synthesized ionic liquid (1-ethyl-3-methylimidazolium bromide, EMIB) as shown in Fig. 3 depicts characteristic molecular ion with the largest relative abundance (m/z) of 120. The predominant peaks identified on the mass spectrum are; peak 1 (propane), peak 9 (bromo-ethane), peak 14 (1- methyl imidazole) and peak 20 (1-ethylimidazole). It was observed that the Peak 9, identified as bromo-ethane was fragmented to m/z =108. The fragmentation was likely due to possible dissipation of a carbon atom from the bromo-ethane chain. Consequent upon fragmentation, a molecule of $C_2H_4N_2$ was also lost from 1-ethylimidazole at peak 20 to form a stable product. Furthermore, the chromatogram presented in Fig. 5 depicted the degradation of certain compounds of the synthesized EMIB. For instance, the nucleophilic attack of the bromide anion was found to be in preference for a methyl group than an ethyl group; hence the formation of bromo-ethane and 1-methylimidazole. This assertion was corroborated by the higher peak (peak 20) recorded for 1-ethylimidazole, compared to those of 1- methyl imidazole (peak 14). Similarly, the cleavage of C - N bond on the ethyl and methyl groups gave rise to ethylene & 1 - methyl imidazole and bromo-ethane & 1-ethylimidazole, respectively.

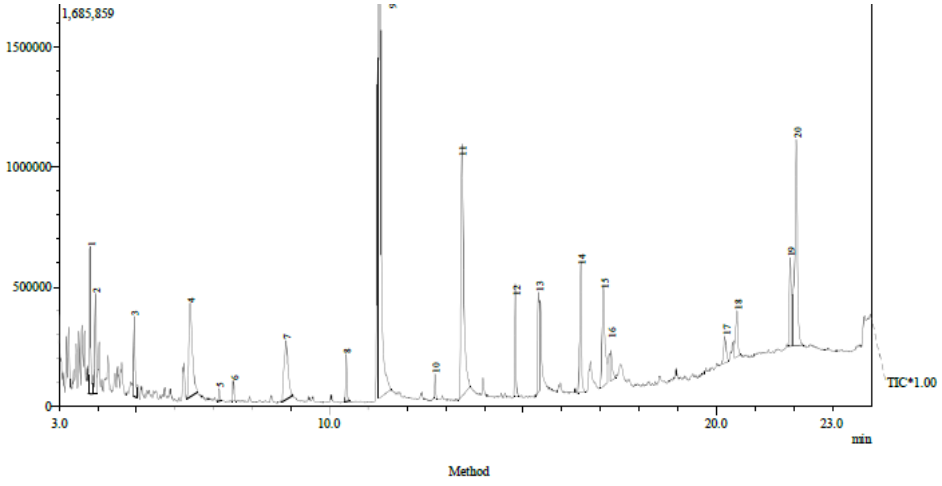

Figure 3. GC-MS image of EMIB

It was notable that the decomposition of imidazole rings, often reflected by the existence of reaction by-products was not deduced from the chromatogram. Therefore, the identification of bromo-ethane and methylimidazole on the chromatogram confirmed that imidazolium-based ionic liquids (EMIB) were successfully synthesized.

3.2. Development of Model Equation

Using multiple regression analysis, the correlation between the four specified independent variables (adsorbent dosage, contact time, effluent temperature and effluent pH) and the response (dephenolation efficiency) was effectively elucidated by a second-order (quadratic) polynomial equation. A representation of the quadratic regression model before elimination of the non-significant terms is shown in Eq. 6. Meanwhile, according to Basu, et al. [17], if given model terms (representation of the respective independent variables) depict probability values (*P*-value) of less than 0.05, the significance of such terms are implied. Such terms are therefore assumed to bear significant effect on the overall response variable. By eliminating the non-significant model terms, the final quadratic response model for the dephenolation operation is given by Eq. 7;

$$Y_{IL-C}(\%) = 98.6 + 0.72X_1 - 2.15X_2 + 2.57X_3 - 2.08X_4 - 0.022X_1X_2 + 0.37X_1X_3 - 0.21X_1X_4 + 1.22X_2X_3 - 0.76X_2X_4 - 0.40X_3X_4 - 1.91X^2_1 - 3.60\,X^2_2 - 1.61\,X^2_3 - 0.40\,X^2_4 \quad (6)$$

$$Y_{IL-C}(\%) = 0.71X_1 - 2.15X_2 + 2.57X_3 - 2.08X_4 + 1.22\,X_2\,X_3 - 0.76\,X_2\,X_4 - 1.91\,X^2_1 - 3.60\,X^2_2 - 1.61\,X^2_3 \quad (7)$$

Where; X_1, X_2, X_3 and X_4 represents the contact time, effluent temperature, dosage and effluent pH, respectively, while Y_{IL-C} is the response variable (dephenolation efficiency). Based on quantitative coefficient (impact factor) of the final regression model expressed in Eq. 7 (X_1 = 0.71, X_2 = 2.15, X_3 = 2.57 and X_4 = 2.08), the order of decreasing priority of the independent variables is adsorbent dosage (X_3) > effluent temperature (X_2) > effluent pH (X_4) > contact time (X_1).

Furthermore, the sign convention of the coefficient value of the terms in the final regression model helps in predicting the nature of the effect of such variable(s) on the overall response. The occurrence of positive coefficient in any of the specified independent variables (in this case, X_1, X_2, X_3, and X_4) suggest that the response variable (dephenolation efficiency) will be favoured by an increase in such variable and vice versa. From Eq. 7, it could be seen that the coefficients of X_2 and X_4 (coded representation for effluent temperature and pH, respectively) have negative sign conventions; thus implying a decrease in dephenolation efficiency with their increase. The reduction in phenol uptake at higher pH could be due to increased solubility of phenol in the aqueous solution, resulting in the production of abundant OH^- ions in the solution which limits the diffusion of phenolate ions onto the adsorbents [18]. Also, the decrease in phenol uptake with temperature rise could be attributed to the weakening of adsorptive forces between the adsorbate (phenol) and the adsorbent occasioned by the increase in kinetic energy due to temperature increase [7].

Similarly, the positive sign conventions of the coefficients of X_1 (coded representation for contact time) and X_3 (coded representation for adsorbent dosage) suggests a possible improvement in the overall output response (dephenolation efficiency) with their increase until equilibrium is attained. This observation concerning contact time is explained by the existence of strong attractive forces between the adsorbates and the adsorbent, thereby resulting in faster diffusion of the phenol molecules into the inter-particle matrices of IL-C as the dephenolation time extended until equilibrium was attained [19]. The increase in dephenolation efficiency with an increase in dosage was expected. This is because the increase in the adsorbents' dose significantly increased the number of adsorbent active sites available for phenol adsorption.

3.3. Statistical analysis

Analysis of variance (ANOVA) was employed to assess the soundness or otherwise of the generated regression model. Such assessment was achieved using various descriptive statistics like probability value (p-value), F-value, coefficient of determination (R^2), adjusted coefficients of determination (R^2_{adj}) and degree of freedom (df). The summary of the ANOVA result was presented in Table 3. Notably, Fischer's F-value and p-value were useful in validating the significance of each model parameter. The F-value compares between the curvature variance and residual variance, while the p-value elucidates the probability of obtaining the observed F-value if the null hypothesis was valid. Meanwhile, a confidence level of 95% ($\alpha = 0.05$) was adopted for determining the statistical significance in all analyses. According to Bayraktar, [20], small probability value ($p < 0.05$) is indicative of a highly significant model, useful for an accurate prediction of the response. Also, the larger and smaller the F-value and p-value is, respectively, the more the significance of the corresponding model term [21].

From Table 3, a relatively large F-values (>> 100) and small p-values (<< 0.05) recorded for model term X_2 – effluent temperature, X_3 – adsorbent dosage and X_4 – effluent pH validates the order of decreasing priority of the independent variables earlier stated in sec. 3.2. The lack of fit test measures the failure of the selected model in representing the predicted data within the experimental domain. The result (Table 3) shows that the lack of fit p-value was greater than 0.05 ($p>0.05$) for the selected model; thus typifying its accuracy in experimental data representation. The goodness of the fit of the model was determined based on the determination coefficient (R^2) value. The R^2 value measures how much of the variability in the observed response values could be explained by the experimental variables and their interactions. The R^2 value is always between 0 and 1. The closer the R^2 value is to 1, the stronger the model and the better its prediction of the response [22]**.** The R^2 value of 0.9873 obtained in the study indicates a high degree of correlation between the observed value and predicted values. This implies that 98.73% of the variations in the dephenolation process were explained by the independent variables and only 1.27% of the total variability in the response was not explained by the model. Furthermore, the "Pred. R^2" of 0.9352 was in reasonable agreement with the "Adjusted R^2" of 0.9755 (within 0.2 numerical differences); thus implying good predictability of the quadratic model [23]**.**

Adequate precision compares the range of predicted values at the design points to the average prediction error. According to Noordin, et al. [24] an adequate precision value greater than 4 is synonymous with selected model adequacy. The adequate precision value of 34.047 (which is far greater than 4) depicted in Table 3, indicates an adequate model efficacy. Considering ANOVA result interpretation concerning standard deviation values, Shrivastava et al. [2] stated that a given model significance is validated if the standard deviation presents a lower value than the mean. Therefore, the low standard deviation value of 0.76 (which is much lower than the mean value) depicted in Table 3 confirms the suitability of the selected model (quadratic model) in correlating the experimental data. The coefficient of variation (CV) indicates the degree of precision with which a given process (in this case, dephenolation) is compared [25]. According to Chowdhury, et al. [26], a CV-values of less than 10 % suggest that the model prediction can be considered reasonably reproducible. From Table 3, the low value of CV (0.81%) indicates great reliability of the dephenolation process. Furthermore, application of the predicted residual sum of squares as a criterion for defining the models' efficiency to predict the responses is captured by the PRESS-value. Katayoon, et al. [27] reported that the smaller the PRESS-value, the more the model significant. PRESS-value of 43.79 (Table 3) corroborates the adequacy and significance of the selected model.

Noteworthy is the fact that the insight derived from the results of all the descriptive statistics discussed in this section aptly demonstrated the high significance, adequacy, accurate predictability and reasonably reproducibility of the selected second-order polynomial regression model.

Table 3. ANOVA for response surface quadratic model

Source	SS	DF	MS	F-value	P-value Prob>F
Model	666.85	14	47.63	83.52	<0.0001 Significant
X_1 – Time	10.48	1	10.48	18.37	<0.0003 Significant
X_2 –Temp	92.55	1	92.55	162.28	<0.0001 Significant
X_3 - Dosage	132.52	1	132.52	232.35	<0.0001 Significant
X_4 –pH	86.90	1	86.90	152.37	<0.0001 Significant
$X_1 X_2$	8.100E-003	1	8.1E-3	0.014	0.9067 insignificant
$X_1 X_3$	2.21	1	2.21	3.87	0.0680 insignificant
$X_1 X_4$	0.70	1	0.70	1.22	0.2863 insignificant
$X_2 X_3$	23.86	1	23.86	41.84	<0.0001 Significant
$X_2 X_4$	9.27	1	9.27	16.26	0.0011 Significant
$X_3 X_4$	2.56	1	2.56	4.49	0.0512 insignificant
X_1^2	33.91	1	33.91	59.46	<0.0001 Significant
X_2^2	121.03	1	121.03	212.22	<0.0001 Significant
X_3^2	24.30	1	24.30	42.61	<0.0001 Significant
X_4^2	1.50	1	1.50	2.63	0.1255 insignificant
Residual	8.55	15	0.57		
Lack of Fit	8.55	10	0.86	15096.2	0.1354
Pure Error	2.83-004	5	0.67E-5		
Core Total	675.40	29			
Std. Dev	0.76		R-Sqr		98.73
Mean	93.59		Adj R-Sqr		97.55
C.V. %	0.81		Pred.R-Sqr		0.9352
PRESS	43.79		Adeq. Precision		34.047

3.4. Analysis of residuals

The normal probability plot of the residuals for the present system is shown in Fig. 4. From the plot, it was observed that the data points were closely distributed along the diagonal line and also depicted a definite "S-shaped" curve pattern. These observations indicate that the model prediction for the dephenolation process was accurate within the limits of the studied range of variables.

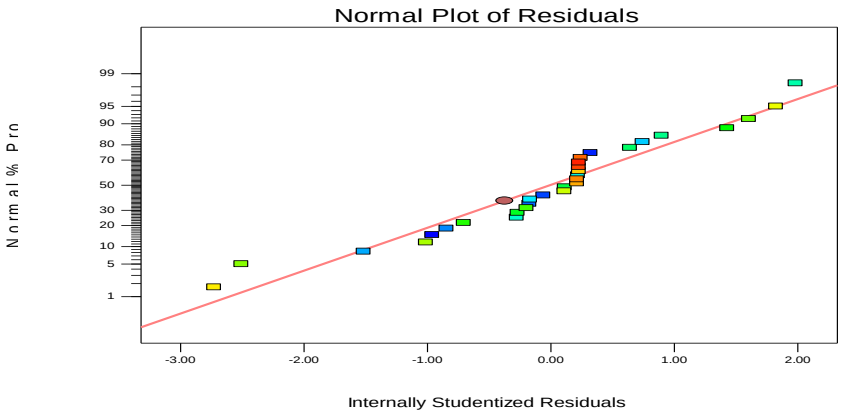

Figure 4. A normal plot of residuals

Similarly, Fig. 5 showed the predicted versus actual plot. This plot helps to identify the values not readily predicted by the model. By visual inspection, it was observed that the data points on Fig. 5 were closely distributed along the diagonal axis. This observation suggests a good correlation between the experimental and predicted response values for the system and further corroborate the correlation between the R^2 and adjusted R^2 values earlier stated in sec 3.3. The seemingly "S" shape curve depicted (along the diagonals) by the data point shown in Fig 5 further confirmed the adequacy of the model for response variable prediction with the independent variables.

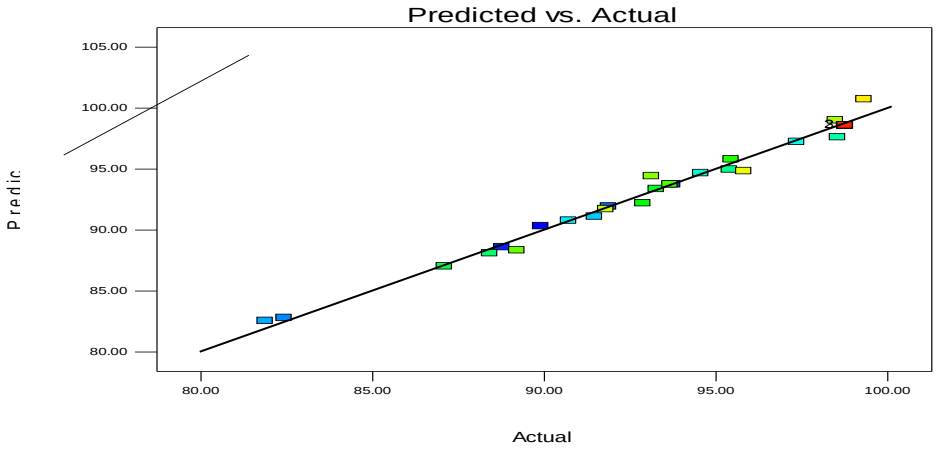

Figure 5. Predicted vs. actual response plot

3.5. Interaction effects of the model terms

From the ANOVA results in Table 3, it was concluded in sec. 3.3 that the independent variables of the quadratic model (contact time, X_1; effluent temperature, X_2; adsorbent dosage, X_3 and effluent pH, X_4) are highly significant. This is because their respective p-values are less than 0.05. Moreover, concerning the interaction effects of the model terms, Table 3 depicted that the interaction between the effluent temperature (X_2) and adsorbent dosage (X_3) and those between effluent temperature (X_2) and effluent pH (X_4) were both significant (because $p << 0.05$). Same could not be said concerning the other model term interaction effects (X_1X_2, X_1X_3, X_1X_4 and X_3X_4), as their respective p-values were in all cases greater than 0.05; hence an insignificant variable interaction. Furthermore, the second-order effect of contact time (X_1^2), effluent temperature (X_2^2) and adsorbent dosage (X_3^2) were all significant because of $p < 0.05$ (Table 3). Meanwhile, the second-order effect of effluent pH (X_4^2) was insignificant because of its corresponding p-value which is >> 0.05.

The Design Expert v8.0 also generated three-dimensional (3D) response surfaces plots which graphically represented the regression equation. Each of the plots presents the response function of two specified variables/factors, with all other factors at a fixed level; thus revealing the activities in the reaction system. The 3D interactive plots for the present system are shown in Fig. 6 (a-b). As stated earlier in sec. 3.2, the independent variables/factors may sustain either a positive or negative effect on the final response variable depending on the sign convention of their respective coefficient values. Similarly, the interaction effect of the variable could also bear a negative or positive effect on the response. The combined influence of pH and time, pH and dosage, temperature and time and dosage and time was observed to be non-significant (see Table

3). Therefore, further discussions regarding their interactive effects, as expressed in the 3D plots were not considered.

Fig. 6(a) shows the combined effect of effluent pH and temperature on dephenolation efficiency. Both variables sustain significant interaction effect on the response variable. The dephenolation efficiency increased with increase in temperature up to 40 ^{0}C and thereafter decreased with further temperature increase regardless of the pH values. Initially, the adsorbate (phenol) required enough kinetic energy to enhance its mobility from the bulk fluid phase into the active sites of the adsorbents. However, beyond 40 ^{0}C as determined in the present study, the increase in kinetic energy due to temperature increase resulted in the weakening of the adsorptive forces between the active sites of the adsorbent and adsorbed molecules. Hence, an optimum temperature of 40 ^{0}C was established in this study. According to Menkiti, et al. [7], further adsorption beyond the optimum temperature threshold will be impossible. Fig. 6(b) shows the combined influence of dosage and temperature on the response variables. A significant interaction between dosage and temperature was observed (see Table 3), thus increase in adsorbent dose led to a corresponding increase in dephenolation efficiency of phenol until saturation (Fig. 6b).

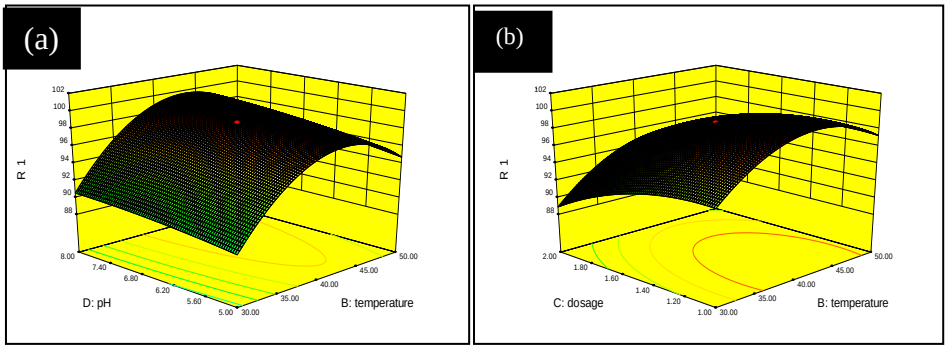

Figure 3. Combined effect of (a) pH and temperature (b) dosage and temperature

3.6. Validation of optimization result

To confirm the model's adequacy for the prediction of maximum dephenolation efficiency (response variable), a replicate experiment was performed using the optimum points of the respective process variables. The obtained result, as presented in Table 4 showed the existence of a good correlation between the predicted and actual dephenolation efficiency at the optimum levels. This is evidenced in their (predicted and actual dephenolation efficiency) close agreement with the validated dephenolation efficiency.

Table 4. Replicate experiments at optimum conditions

Parameter	Optimum values	Actual dephenolation efficiency (%)	Model predicted dephenolation efficiency (%)	Validated dephenolation efficiency (%)
Contact time (min)	25	97.15	98.50	98.34
Temperature (^{0}C)	40	-	-	-
Adsorbent dose (g)	1.5	-	-	-
Effluent pH	6.5	-	-	-

*NB: The actual, predicted and validated efficiency was uniform for all parameters, hence the Dash (-) notation.

4. CONCLUSION

The present study has demonstrated the usefulness of response surface methodology in the modelling and optimization of the adsorption process of phenol from petroleum wastewater. The optimum conditions and the interaction effects of the process variables (temperature, pH, contact time, and adsorbent dose) were determined. It was observed that phenol removal efficiency was significantly affected by dosage, pH and temperature. Furthermore, Second-order polynomial regression model successfully elucidated the effect of the independent variables on the dephenolation process, with a coefficient of determination (R^2) value of 0.98. The process optimization revealed that the optimum operating condition for realizing the maximum removal efficiency (91.67 %) was; 25 min, 40 ^{0}C, pH 6.6 and 1.5g adsorbent mass.

Declaration of interests

The authors declare that they have no known competing financial interests or personal relationships that could have appeared to influence the work reported in this paper.

REFERENCES

[1] WHO (1994). IPCS Environmental health criteria for phenol first draft prepared by Montizan GK, Published by WHO. Printed in Finland.

[2] Shrivastava, V.C., Swamy, M.S., Mall, I.D., Prasad, B., & Mishra, I.M. (2006). Adsorptive removal of phenol by bagasse fly ash and activated carbon: equilibrium, kinetics and thermodynamics. *Colloid Surf. A.,* 272, 89–104.

[3] Ahmaruzzaman, M. (2008). Adsorption of phenolic compounds on low-cost adsorbents: a review, *Adv. Colloid Interface Sci*., 143(1), 48-67.

[4] Sunil, J., Kulkarni., D., & Jayant, P.K. (2013). Review on research for removal of phenol from wastewater. *International Journal of Scientific and Research Publications,* 3, (4).

[5] Song, X., Zhang, Y., Yan, C., Jiang, W., & Chang, C. (2013). The Langmuir monolayer adsorption model of organic matter into effective pores in activated carbon. *Journal of Colloid and Interface* Sci., 389(1), 213–219.

[6] Kadhimand, F., & Al-Seroury F.A. (2012). Characterization the removal of phenol from aqueous solution in fluidized bed column by rice husk adsorbent, *Research Journal of Recent Sciences*, (1), 145–151.

[7] Menkiti, M.C., Abonyi, M.N., & Aniagor, C.O. (2018). Process equilibrium, kinetics and mechanisms of ionic-liquid induced dephenolation of petroleum effluent. *Water Conserv. Sci. Eng.*, 3, 205–220. https ://doi.org/10.1007/s4110 1-018-0052-8.

[8] Abonyi, M. N., Aniagor, C. O., & Menkiti, M. C. (2019). Effective Dephenolation of Effluent from Petroleum Industry Using Ionic-Liquid-Induced Hybrid Adsorbent. *Arabian Journal for Science and Engineering.* https://doi.org/10.1007/s13369-019-04000-8

[9] Chatterjee, S., Kumar, A., Basu, S., & Dutta, S. (2012). Application of response surface methodology for methylene blue dye removal from aqueous solution using low-cost adsorbent. *Chemical Engineering Journal*, 181 – 182, 289 – 299.

[10] Mohammad, Y.S., Shaibu-Imodagbe, E.M., Igboro, S.B., Giwa, A., & Okuofu, C.A. (2014). Modelling and Optimization for Production of Rice Husk Activated Carbon and Adsorption of Phenol. *Journal of Engineering.* http://dx.doi.org/10.1155/2014/278075

[11] Wilkes, J. S., & Zaworotko, M. J. (1992). Air and water stable 1-ethyl-3-methylimidazolium based ionic liquids, *J. Chem. Soc., Chem. Commun.*, 8(3), 965-967.

[12] Aniagor C.O. & Menkiti M.C. (2018). Kinetics and mechanistic description of adsorptive uptake of crystal violet dye by lignified elephant grass complexed isolate. Journal of Environmental Chemical Engineering. 6, 2105–2118. https://doi.org/10.1016/j.jece.2018.01.070

[13] Zainudin, N.F., Lee, K.T., Kamaruddin, A.H., Bhatia, S., & Mohamed, A.R. (2006). Study of adsorbent prepared from oil palm ash (OPA) for the gas desulphurisation. *Separation purification technology*, 97, 734-739.

[14] Stuart, B., (2004). *Infrared Spectroscopy: Fundamentals and Applications.* Hoboken, New Jersey: John Wiley & Sons

[15] Madejova, J. (2003). FTIR techniques in clay mineral studies. *Vibrational Spectroscopy*, 31, 1-10.

[16] Chang, R. (2005). *Physical Chemistry for the Biosciences*, University Science Books, NY, USA.

[17] Basu, J.K, Monal, D., & Pinaki, G. (2012). Chitosan-immobilized Optimization of electrocoagulation process for removal of phenol. *Archives of Applied Science Research*, 4(2), 1053 - 1060.

[18] Liu, X; & Pinto, N.G. (1997). Ideal adsorbed phase model for adsorption of phenolic compounds on activated carbon. *Carbon*, 35(9), 1387-1397. https://doi.org/10.1016/S0008-6223(97)00092-4

[19] Sathishkumar, M., Binupriya, A.R., Vijayaraghavan, K., & Yun, S. I. (2007). Two and three-parameter isothermal modelling for liquids-phase sorption of procion blue HB by inactive mycelia biomass of *panus fulvus. Journal of chemical technology and biotechnology,* 82, 389-398.

[20] Bayraktar, E. (2001)**.** Response surface optimization of the separation of DL-tryptophan using an emulsion liquid membrane. *Process Biochem.*, 37, 169–175.

[21] Dorra, T., Soumaya, H., Islem, L., & Bachir, H. (2017). Response surface methodology for optimization of phenol adsorption by activated carbon: Isotherm and kinetics study. *Indian journal of chemical technology*, 24, 239-255.

[22] Chandana, L.M., Sridevi, V., Narasimha, R.M., & Swamy, A. (2011). Optimization of phenol degradation from pseudomonas aeruginosa (ncim 2074) using response surface methodology. *International Journal of research in pharmacy and chemistry*. 1(4).

[23] Ray, S., Lalman, J.A., & Biswas, N. (2009). Using the Box-Benkhen technique to statistically model phenol photocatalytic degradation by titanium dioxide nanoparticles. *Chemical Engineering Journal*, 150, 15–24.

[24] Noordin, M.Y., Venkatesh, V.C., Sharif, S., Elting, S., & Abdullah, A. (2004). Application of response surface methodology in describing the performance of coated carbide tools when turning AISI 1045 steel. *Journal of Mater. Process Technology*, 145, 46–58.